Academic Journal of Science and Technology
ISSN: 2771-3032 | Vol. 15, No. 1, 2025

Improvement of the Fault Intensity Index Calculation Method Based on High-density 3D Seismic Exploration Results

Lei Han[1], Dongchun Zhao[2], Meng Zhang[2], Liliang Luo[2], Jiangfeng Chen[1, *]

[1]College of Resource and Environment, Henan Polytechnic University, Jiaozuo, China
[2]Henan Shenhuo Coal and Electricity Limited Liability Company Liu He coal mine, Shangqiu, China
[*]Corresponding Author: CHEN Jiangfeng

Abstract: Structural quantification serves as a critical task in evaluating mine water hazards and structural complexity. The selection of quantification methodologies significantly impacts the authenticity and precision of mine-related assessments. To address the limitation of conventional Fault Strength Index (FSI) calculations, which approximate fault morphology as rectangular geometries—leading to discrepancies between calculated FSI values and actual fault developmental characteristics—this study focuses on the No. 32 Mining Panel of Liangbei Coal Mine. Utilizing high-density 3D seismic exploration data and inversion results of faults within the study area, fault throws exceeding 5 m were calculated at discrete points along fault extensions via the interpolation method applied to coal seam floor contour maps. Based on the morphological characteristics of faults depicted in geological graphics, optimal coordinate points were selected to establish a 2D coordinate system. Fault extension lengths and throw values were then processed into 2D coordinates. MATLAB's curve-fitting toolbox was employed to derive fitting equations describing the relationship between fault throw and extension length. An improved FSI calculation method was proposed by integrating fault fitting functions into the quantification framework. Comparative analysis with traditional FSI results demonstrates that the enhanced methodology better aligns with the actual developmental morphology of faults. This refinement not only resolves subjective biases inherent in conventional rectangular approximations but also establishes a more robust foundation for structural complexity zoning and hydrogeological risk management in underground mining environments.

Keywords: Fault intensity index, Fitting, integration, Quantitative analysis.

1. Introduction

The complexity of geological structure is one of the important factors affecting water inrush and safe mining in coal mines, and scientific and reasonable quantification of structural complexity is of great significance to guide the safe production of mines [1-3]. The key points of quantitative evaluation of the complexity of mine structure are divided into two aspects: evaluation index and evaluation model [4-7]. In recent years, the quantitative evaluation of the complexity of mine structures has achieved many achievements in practice, and the fault fractal dimension and fault strength index have become good indicators for evaluating the complexity of structures [8-11]. Although the fault strength index can well reflect the complexity of the fault in three-dimensional space, this method has the disadvantage of simplifying the fault plane into a rectangle in the quantization process. In view of the shortcomings of this method in calculating the fault strength index, this paper uses fitting integral to improve the original calculation method, so that the fault strength index can be more in line with the actual development of the fault.

At present, 3D seismic exploration technology is one of the most effective technical means to obtain geological structure characteristics of mines, identify small faults, goaf and target coal seam distribution [12,13]. With the development of seismic exploration technology and the continuous improvement of exploration requirements, today's high-density 3D seismic exploration can identify small faults within 5 m in coal seams through fine data processing technology [14,15]. In practical engineering applications, after technical processing of high-density 3D seismic exploration, the identification accuracy of fault with a drop greater than 3 m and collapse column with a long axis greater than 30 m is close to 80%[16]. On the basis of the exploration results obtained by high-density 3D seismic, this paper fits the curve equation between the horizontal extension length of the fault and the drop with the help of MATLAB, improves the calculation formula of the fault strength index, and realizes the accurate quantification of the fault in the study area by integrating the fitting function.

2. Calculation Method and Improvement of Fault Strength Index

2.1. Fault strength index

The Fault Strength Index is the most widely used fault quantification method at present. It quantifies faults by calculating the sum of the product of all fault extension lengths and their own falls within a unit area. Compared with fault density index and fault length index, fault intensity index can better reflect the complexity of faults in three-dimensional space . Its calculation formula is as follows:

$$F = \frac{\sum_{i=1}^{n} L_i H_i}{S} \quad (1)$$

Where:
F: Fault Strength Index;

n: Number of faults within the statistical unit;

L_i: Horizontal extension length of the i-th fault in the statistical unit (m);

H_i: Throw of the i-th fault in the statistical unit (m);

S: Area of the statistical unit (m^2).

This formula integrates both geometric and kinematic attributes of faults, offering a robust metric for evaluating structural complexity in coal mine geology. By incorporating fault throw and extension length, the FSI effectively bridges the gap between planar fault representations and their true 3D developmental patterns, making it indispensable for hydrogeological hazard assessments and mining design optimization.

2.2. Improvement of fault strength index

On the basis of fault inversion data obtained by 3D seismic exploration, the drop of each fault at different positions along the fault extension direction and the corresponding horizontal distance of the coal crossing line of the upper and lower panel were obtained, the fault function equation was fitted, and the improved fault strength index calculation formula (2) was used for calculation, so as to achieve accurate quantification of the fault.

$$F = \frac{\sum_{i=1}^{n} \int_{x_1}^{x_2} f_i(x)\,dx}{S} \tag{2}$$

Where:

x_1,x_2: Integration limits corresponding to the starting and ending points of the fault extension length within the statistical unit (m);

$fi(x)$:Fitting function characterizing the relationship between throw and extension length for the i-th fault in the statistical unit;

3. Overview of the Study Area

The study area is the 32 mining area of Liangbei Coal Mine, the strata in this area is a monoclinal structure, and the strata developed from old to new successively include the Cambrian Changshan Formation, the Carboniferous Taiyuan Formation, the Permian Shanxi Formation, the upper and lower Shihezi Formation, the Sunjia Formation and the Quaternary system. The main coal seam that can be mined is 2 1 coal, which exists at the bottom of Shanxi Formation, with a storage elevation of 0 ~ -800 m, a burial depth of 115 ~ 1017 m, and a stable bedding. According to the 3D seismic exploration results of 21 coal seam, the fracture structure is relatively developed, and 36 faults are identified (fig. 1). There are 35 normal faults and 1 reverse fault.

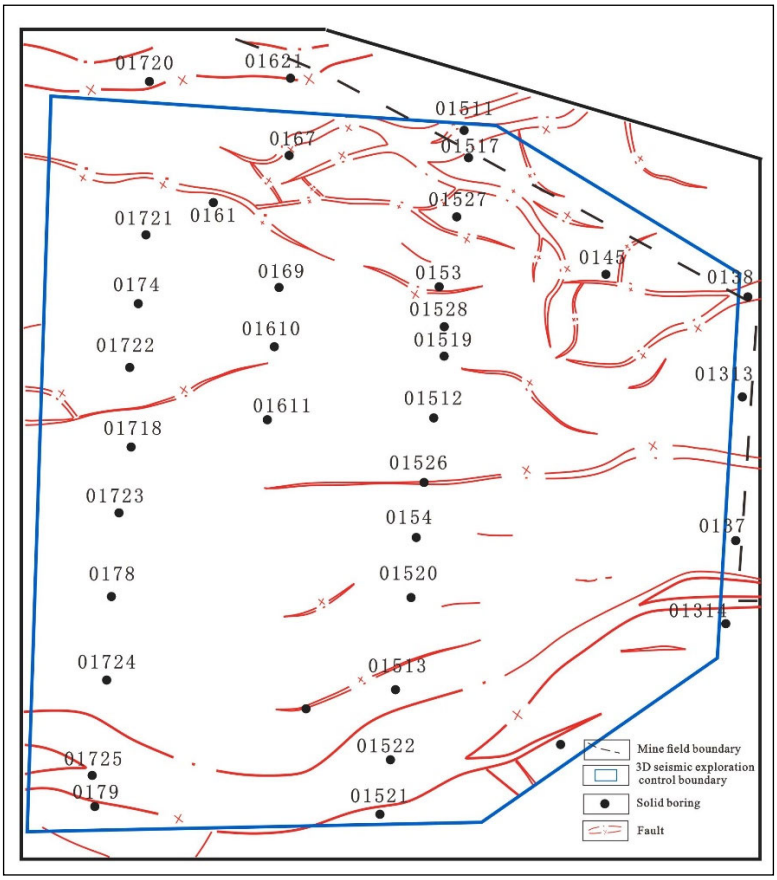

Figure 1. 3D seismic interpretation of the study area coal seam floor fault distribution map

4. Research Methodology

In the 3D seismic exploration results of coal seam floor, affected by fault structure, the elevation value of the coal seam floor's broken coal crossing line will shift through the cutting of the fault, and the difference value of the coal seam floor's broken coal crossing line elevation on the same layer site is the drop value of the fault at that layer site. Under normal circumstances, the smaller the dip Angle of the fault and the larger the drop, the larger the horizontal distance of the coal crossing line of the upper and lower plate. Therefore, by determining the maximum point of the horizontal distance

between the upper and lower panel fault lines in the 3D seismic contour map of coal seam floor in the study area, the maximum point of the horizontal distance between the upper panel fault lines is not only the maximum point of the fault drop, but also the inflection point of the change of the fault drop. Taking the maximum drop point of fault as the base point, several control points controlling the change of the drop curve between the base point and the two ends are determined, and the drop value of each fault control point is calculated by the difference of the contours of the coal crossing line of the upper and lower panel. The obtained data are statistically sorted out, and the origin of the two-dimensional coordinate system is determined by finding suitable position points in the fault extension trajectory. The distance from the fault endpoint, control point and maximum drop point to the coordinate origin is respectively measured as the horizontal coordinate data, and the drop value of each point is taken as the longitudinal coordinate data. The obtained two-dimensional coordinate data was imported into MATLAB software for fitting, the curve equations of each fault were fitted, and the fault strength index in the study area was calculated using equation (2).

5. Data Statistics and Processing

Taking the F201 fault in the study area as an example, this fault exhibits a maximum vertical throw of 24 m with an extension length of 725 m (Figure 2). Based on the interpretation results from the 3D seismic exploration contour map of the No. 2-1 coal seam floor regarding the F201 fault, and according to the relationship between the horizontal separation of upper/lower wall coal-seam intersection lines versus fault throw and dip angle, we determined the maximum throw location along the fault plane by identifying the maximum horizontal separation value of coal-seam intersection lines. The control points for the fault throw curve were established through analyzing variation amplitudes of horizontal separation values between upper and lower walls, with fault throw at each control point calculated using interpolation methods based on coal seam floor elevation contour values.

Seven control points were identified for the F201 fault, including two endpoints at fault extremities, one maximum throw point, and four inflection points reflecting throw variations along the fault strike. A coordinate system was established with the left endpoint as the origin (X-axis along strike direction towards the right endpoint, Y-axis representing vertical throw). The coordinates of these seven control points were input into MATLAB software to perform curve fitting, deriving the functional relationship between fault throw and extension length. Figure 3 illustrates the fitting results, where the black solid line represents actual throw variations and the blue dashed line shows the fitted curve with R^2=0.9853, indicating excellent correlation. This confirms the fitted curve equation effectively describes the throw-extension relationship.

Following this methodology, similar curve fitting was conducted for all faults with throws exceeding 5 m within the study area. The resulting fitting equations for each fault are summarized in Table 1.

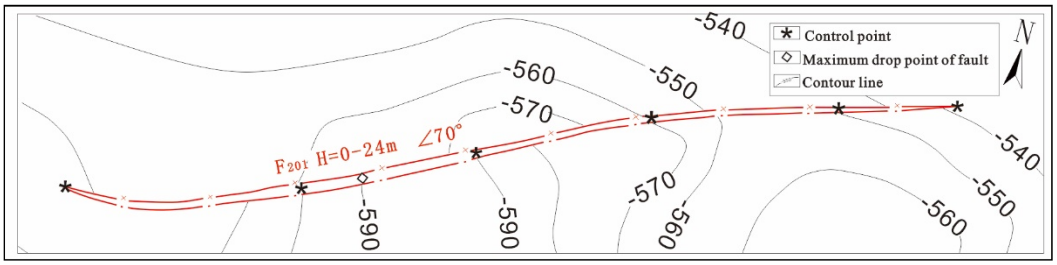

Figure 2. F_{201} fault 3D seismic exploration interpretation results Structural outline map of the study area

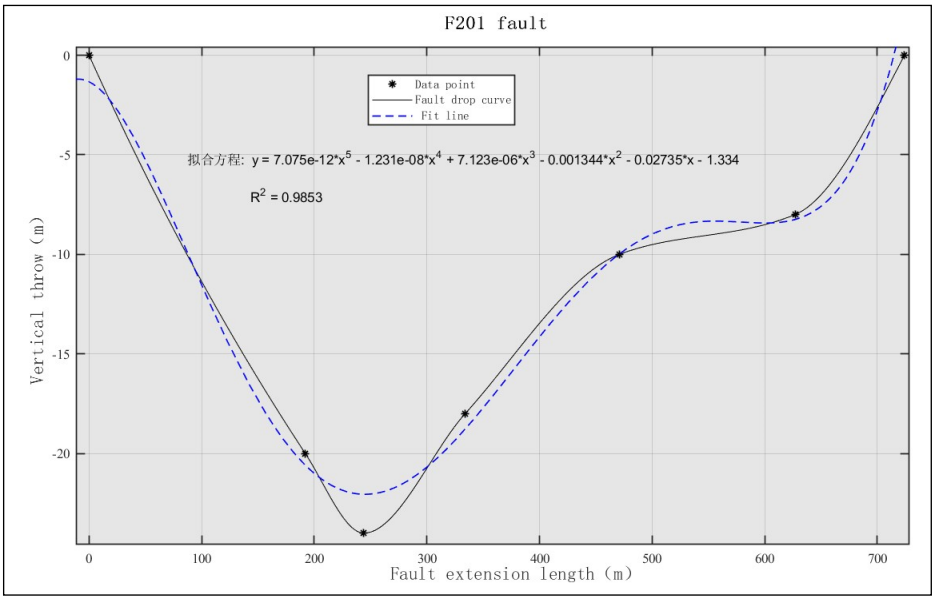

Figure 3. F_{201} fault fitting results

Table 1. Fault fitting function table in the study area

Fault name	Fit the functional equation	R^2
F_2	$y = 0.0001715*x^2 - 0.1095*x - 178$	0.9334
F_{14}	$y = (4.527*10^{-10})*x^4 - (1.172*10^{-6})*x^3 + 0.001151*x^2 - 0.4746*x + 18.87$	0.9552
DF_{10}	$y = (2.706*10^{-10})*x^4 – (6.145*10^{-7})*x^3 + 0.0005489*x^2 - 0.1792*x - 13.82$	0.9906
DF_{24}	$y = 0.0004785*x^2 - 0.1973*x - 0.7728$	0.9948
DF_{12}	$y = 0.0008743*x^2 - 0.2223*x + 0.1249$	0.9993
DF_9	$y = 0.0005743*x^2 - 0.216*x + 2.918$	0.9686
F_{2-3}	$y = 0.000247*x^2 - 0.1731*x - 6.748$	0.9385
F_{2-1}	$y = - (7.842*10^{-7})*x^3 + 0.0007117*x^2 - 0.268*x + 3.762$	0.9752
DF_6	$y = 0.01638*x^2 - 3.023*x - 8.038$	0.9903
DF_5	$y = 0.0002375*x^2 - 0.1229*x - 0.09903$	0.9998
F_{17-2}	$y = 2.73*10^{-7}*x^3 - 0.0003743*x^2 + 0.1422*x - 22.57$	0.9392
DF_3	$y = - (1.304*10^{-6})*x^2 - 0.03562*x + 0.5316$	0.9952
DF_{28}	$y = 0.000935*x^2 - 0.2449*x - 1.246$	0.9852
DF_8	$y = 0.002879*x^2 - 0.3029*x - 0.035$	0.9999
DF_{31}	$y = 0.001673*x^2 - 0.2178*x + 0.08056$	0.9986
F_{201}	$y = (7.075*10^{-12})*x^5 – (1.231*10^{-8})*x^4 + (7.123*10^{-6})*x^3 - 0.001344*x^2 - 0.02735*x - 1.334$	0.9853
DF_2	$y = 3.212*10^{-6}*x^3 - 9.355e\text{-}06*x^2 - 0.148*x - 1.297$	0.9763
DF_{27}	$y = 0.0003802*x^2 - 0.1311*x + 0.2043$	0.9919
DF_{29}	$y = 0.0004193*x^2 - 0.1612*x + 0.2507$	0.9858
DF1	$y = - 0.06283*x + 0.814$	0.9979
DF_{21}	$y = 0.0002889*x^2 - 0.1018*x - 3.225$	0.9936
DF_{18}	$y = 0.001639*x^2 - 0.1991*x + 0.04428$	0.9995
F_{2-2}	$y = 0.0002112*x^2 - 0.3266*x + 5.057$	0.9675
F_{05}	$y = 0.0001344*x^2 - 0.1947*x + 5.738$	0.9497
DF_{11}	$y = - 0.0972*x + 0.4389$	0.9979
DF_{25}	$y = 0.0006661*x^2 - 0.2033*x + 0.2213$	0.9831
F_1	$y = - (7.275*10^{-11})*x^4 + (4.022*10^{-7})*x^3 - 0.0006191*x^2 + 0.1877*x - 185.8$	0.9697
DF_{23}	$y = 0.002409*x^2 - 0.3545*x - 9.963$	1.00
DF_7	$y = -(4.641*10^{-6})*x^3 + 0.002945*x^2 - 0.5016*x + 1.443$	0.9949

6. Results and Analysis

A statistical grid system with 300 (m) × 300 (m) cells was established across the study area. Fault intensity indices were calculated using Equations (1) and (2), and central coordinates of each grid cell were extracted to generate fault intensity index contour maps via Surfer software, as shown in Figure 4.

The maximum fault intensity index calculated by the traditional method was 1.4, while the improved method yielded a maximum value of 1.2. For instance, the DF3 fault exhibits a maximum vertical throw of 70 m on the right side of the study area. However, its maximum throw decreases to 30 m within a 1000 m extension range toward the left endpoint. The traditional method produced a fault intensity index of 0.25 in this range (Figure 4a), whereas the improved method resulted in 0.047 (Figure 4b). Comparative analysis of the F1 fault calculations reveals that the traditional method tends to overestimate large faults due to inherent limitations. In contrast, the improved method employs integral calculations based on fault throw fitting functions, eliminating subjective biases and yielding results that better reflect actual fault development characteristics, thereby demonstrating superior accuracy.

By incorporating linear fitting relationships of fault throw variations, the improved method minimizes subjective influences and effectively distinguishes zones of differential fault displacement. Compared to the traditional approach, it provides a more objective partitioning of structural complexity across the study area.

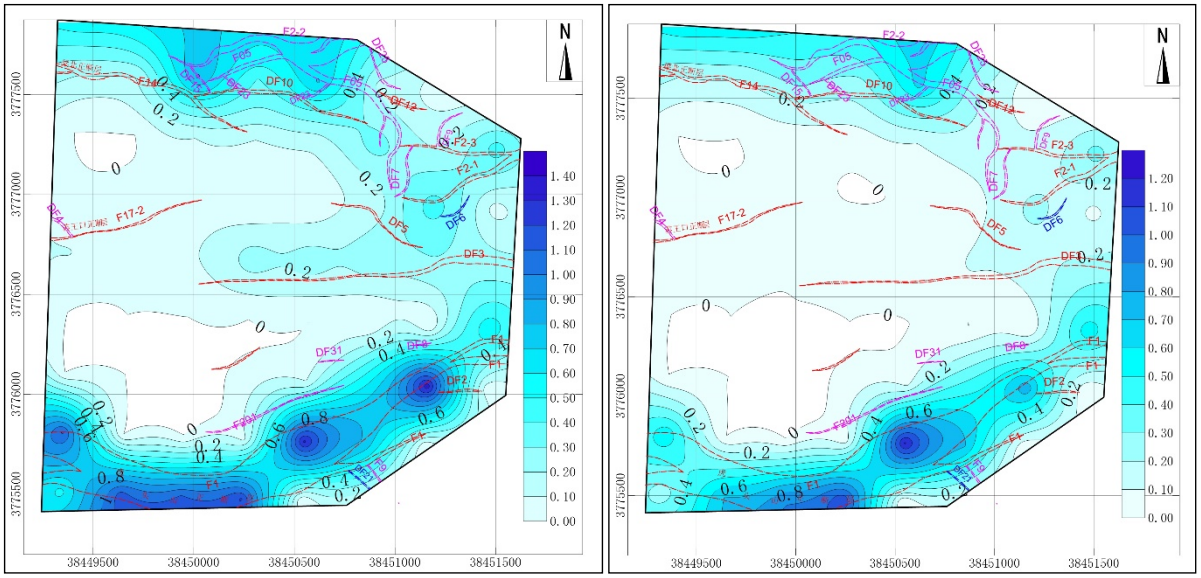

a. Calculation results of conventional methods b. Improved method calculation results

Figure 4. Contour map of fault strength index in study area

7. Conclusions

(1) Compared with conventional fault strength index calculation methods, the improved methodology employing fitted functional equations derived from fault throw and extension length data within uniform statistical cells demonstrates superior alignment with fault developmental morphology. This approach eliminates subjective influences during data processing and effectively differentiates fault development heterogeneity through quantitative characterization, providing an alternative paradigm for structural quantitative zoning.

(2) Precise quantification of fault planes not only enhances the accuracy of fault structure complexity evaluations, but also enables three-dimensional spatial extrapolation from two-dimensional fitting results. This advancement holds significant guidance value for grouting operations targeting water blockage within fault zones, offering enhanced engineering applicability in underground hydrological management.

References

[1] SHI Longqing, LIU Jie, QIU Mei, et al. Application of fault quantification in risk assessment of water inrush[J]. China Sciencepaper, 2020,15(01):100-104+130.

[2] XU Fengyin, LONG Rongsheng, XIA Yucheng, et al. Quantitative assessment and prediction of geological structures in coal mine[J]. Jouranl of China Coal Society, 1991, (04):93-102.

[3] XU Fengyin, WANG Guiliang, ZHU Xingshan, et al. Some difficult problems and their preliminary research in the quantitative forecast of geological structure in coal mine[J]. Coal Geology & Exploration, 1992,(01):27-33.

[4] ZHOU Yunxia, CAO Daiyong. Quantitative evaluation model of mine geological structure[J]. Coal Geology & Exploration, 2001, (02):16-19.

[5] XU Fengyin, LONG Rongsheng, XIE Gaowen, et al. Evaluation index and research method in quantitative prediction of mine geological structure[J]. Mining Safety & Environmental Protection, 1991,(05):21-25.

[6] XIA Yucheng, FAN Huairen. The principles and methods of quantitative assessment of mine structure[J]. Journal of Xi'an University of Science and Technology, 1998,(04):323-327.

[7] XIA Yucheng. Advance of quantitative prediction method of mine structure[J]. Geology and Exploration, 2001,(03):61-63.

[8] XIA Yucheng, JIA Haili. Qutomatic quantitative technique to predict relative complexity degrees of mine structure[J]. Journal of China Coal Society, 2000,(S1):22-25.

[9] CHEN Jiangfeng, ZHU Zhijun, YAN Changde. Fractal dimension description of fault density in coal mine[J]. Coal Geology of China, 1999,(03):8-10+21.

[10] XU Zhibin, WANG Jiyao, ZHANG Dashun, et al. Fractal dimension description of complexity of fault network in coal mine[J]. Journal of China Coal Society, 1996,(04):24-29.

[11] SHI Longqing, ZHAO Wei, LIU Tianhao, et al. Quantitative evaluation for structure complexity of coal mine field[J]. Coal Engineering, 2022,54(08):142-148.

[12] GAO Yuan, WANG Qi, DONG Shouhua, et al. The technology of 3D prestack depth migration an its application[J]. Coal Geology & Exploration, 2011,39(03):71-73.

[13] DONG Shouhua, HUANG Yaping, JIN Xueliang, et al. Development status and trend of high-density 3D seismic exploration technology for coal fields[J]. Coal Geology & Exploration, 2023,51(02):273-282.

[14] JIN Xueliang, WANG Qi. Pattern and effect of the density 3D seismic exploration in coal mining districts[J]. Coal Geology & Exploration, 2020,48(06):1-7+14.

[15] XING Tao, HAN Jianguang, ZHU Guanghui, et al. Application of 3D seismic fine processing technology in identifying small fault in coalfields[J]. Geological Review, 2023,69(02):615-624.

[16] LI Jingtao, WANG Wei. High-density 3D seismic prospecting serving and its effects analysis in intelligent working face[J]. Coal Technology, 2024,43(01):96-101.